European Journal of Radiology Open 6 (2019) 49–55

Contents lists available at ScienceDirect

European Journal of Radiology Open

journal homepage: www.elsevier.com/locate/ejro

Can apparent diffusion coefficient values help distinguish between different types of pediatric brain tumors?

Abdulaziz Mohammad Al-Sharydah[a,*], Hussain Khalid Al-Arfaj[b], Husam Saleh Al-Muhaish[b], Sari Saleh Al-Suhaibani[a], Mohammad Saad Al-Aftan[a], Dana Khaled Almedallah[c], Abdulrhman Hamad Al-Abdulwahhab[a], Abdullah Abdulaziz Al-Hedaithy[c], Saeed Ahmad Al-Jubran[a]

[a] Radiology Department, Imam Abdulrahman Bin Faisal University, King Fahd Hospital of the University, Al-Khobar City, Eastern Province, Saudi Arabia
[b] Medical Imaging Department, King Fahad Specialist Hospital, Dammam City, Eastern Province, Saudi Arabia
[c] College of Medicine, Imam Abdulrahman Bin Faisal University, Dammam City, Eastern Province, Saudi Arabia

ARTICLE INFO

Keywords:
Apparent diffusion coefficient
Differential diagnosis
Magnetic resonance imaging
Pediatric brain tumor

ABSTRACT

Rationale and objectives: Classifying brain tumors is challenging, but recently developed imaging techniques offer the opportunity for neuroradiologists and neurosurgeons to diagnose, differentiate, and manage different types of brain tumors. Such advances will be reflected in improvements in patients' life expectancy and quality of life. Among the newest techniques, the apparent diffusion coefficient (ADC), which tracks the rate of microscopic water diffusion within tissues, has become a focus of investigation. Recently, ADC has been used as a pre-operative diffusion-weighted magnetic resonance imaging (MRI) parameter that facilitates tumor diagnosis and grading. Here, we aimed to determine the ADC cutoff values for pediatric brain tumors (PBTs) categorized according to the World Health Organization (WHO) classification of brain tumors.

Materials and methods: We retrospectively reviewed 80 cases, and assessed them based on their MRI-derived ADC. These results were compared with those of WHO classification-based histopathology.

Results: Whole-lesion ADC values ranged $0.225–1.240 \times 10^{-3}$ mm^2/s for ependymal tumors, $0.107–1.571 \times 10^{-3}$ mm^2/s for embryonal tumors, $0.1065–2.37801 \times 10^{-3}$ mm^2/s for diffuse astrocytic and oligodendroglial tumors, $0.5220–0.7840 \times 10^{-3}$ mm^2/s for other astrocytic tumors, and $0.1530–0.8160 \times 10^{-3}$ mm^2/s for meningiomas. These findings revealed the usefulness of ADC in the differential diagnosis of PBT, as it was able to discriminate between five types of PBTs.

Conclusion: The application of an ADC diagnostic criterion would reduce the need for spectroscopic analysis. However, further research is needed to implement ADC in the differential diagnosis of PBT.

1. Introduction

Pediatric central nervous system tumors are rarely seen in clinical practice globally. Surprisingly, however, they account for the second most frequent type of cancer in Saudi Arabia, after leukemia, and are most common among males [1]. It has been reported that 90% of these tumors are intracranial, and half of them are found in the posterior fossa in pediatric patients [2]. They are often difficult to manage suitably due to diagnostic complexities, which would involve analytical interpretations of multiple magnetic resonance imaging (MRI) sequences covering a wide array of imaging features and histological morphologies [3]. Therefore, classifying brain tumors is challenging. It would be important to provide neuroradiologists and neurosurgeons with a differential diagnosis tool that could help in the diagnosis and management of these cases, and hopefully improve patients' life expectancy and quality of life.

Diffusion-weighted MRI is a technique that tracks the random Brownian motion of water particles at the microscopic level within biological tissues. The apparent diffusion coefficient (ADC) can be determined based on diffusion-weighted images [4,5], and has been used as a preoperative parameter that allows tumor diagnosis and grading [5]. Raisi-Nafchi et al. [6] reported an inverse relationship between the histopathological grade of glial tumors and the minimum apparent diffusion coefficient (ADCmin). This is attributed to the fact that an

* Corresponding author at: Radiology Department, King Fahd Hospital of the University, Imam Abdulrahman Bin Faisal University, P.O. Box: 31952 (4398), Al-Khobar City, Eastern Province, Saudi Arabia.
E-mail address: amsharydah@iau.edu.sa (A.M. Al-Sharydah).

https://doi.org/10.1016/j.ejro.2018.12.004
Received 9 October 2018; Accepted 17 December 2018
Available online 04 January 2019

increase in cellularity increases nuclear-to-cytoplasmic ratios and decreases extracellular space in higher-grade lesions, restricting water diffusion, and vice versa [7–9]. Therefore, restricted diffusion has now been demonstrated to correspond with the grading of high-grade cerebral tumors in pediatrics [10].

In addition, several reports have proposed the use of ADC values to distinguish between different histologically variable brain tumors in pediatric patients [11,12]. Erdem et al. [13] further emphasized the role of average ADC values in the diagnosis of posterior fossa tumors in children. One other study suggested that ADC could potentially be used as a pre-diagnostic measure for predicting brain tumor histopathology [14].

Overall, however, there have been only few studies on the diffusion-weighted image characteristics of pediatric patients, with some studies focusing exclusively on a particular anatomical lesion, such as the posterior fossa or the cerebellum, while others have included small sample sizes [15–18]. Moreover, there has been an extensive overlap of ADC value intervals across different classification groups and criteria, without clear cutoff values [15].

Thus, further investigation is needed to determine the ADC cutoff values for pediatric brain tumors (PBTs). Here, we aimed to determine such cutoff values based on the World Health Organization (WHO) classification of brain tumors [19], which uses molecular parameters in addition to analytical histopathology to define many tumor entities, thus formulating a precise diagnosis of brain tumors. This article provides evidence towards the application of ADC as a diagnostic criterion for PBT.

2. Materials and methods

2.1. Study setting

This study was conducted at King Fahd Hospital of the University, Imam Abdulrahman Bin Faisal University, Eastern Province, Saudi Arabia, an academic tertiary governmental hospital with a capacity of 600 beds.

2.2. Study design and patients

We used the keyword “brain tumor,” of the ICD-9 coding system, as well as codes 191.9, 225.0, and 239.6 for benign, malignant, and unspecified brain tumors, respectively, to obtain pathology reports of interest from the electronic medical files of King Fahd University hospital. Next, a review of the radiology database was conducted to screen data collected over the past 10 years. We eventually retrospectively reviewed 117 patients diagnosed with a histopathologically confirmed PBT, on whom brain imaging studies had been performed between March 2016 and June 2017.

2.3. Inclusion and exclusion criteria

Only lesions measuring more than 1 cm in diameter on MRI and confirmed by histopathology were included. We excluded cases of pseudotumors and cases that lacked diffusion-weighted/ADC signals in their imaging protocol. From the subsequent statistical analysis, we excluded cases with an insufficient sample size for comparison or with missing data. In total, we excluded 37 cases of choroid plexus tumors, mesenchymal and nonmeningothelial tumors, tumors of the sellar region, and tumors of the pineal region. Therefore, based on the WHO classification system for brain tumors [19], we included five types of PBT, namely diffuse astrocytic and oligodendroglioma tumors (49 cases), other astrocytic tumors (7 cases), embryonal tumors (12 cases), ependymal tumors (5 cases), and meningiomas (7 cases).

2.4. Histopathological reports

The following types of tumors were diagnosed based on histopathology. (A) Supratentotrial tumors: glioblastoma multiforme (n = 27), anaplastic oligodendroglioma (n = 6), low-grade glioma (n = 4), craniopharyngioma (suprasellar) (n = 2), neuroblastoma (metastasis) (n = 2), porencephalic cyst (n = 2), melanotic neuroectodermal tumor (n = 1), adamantinomatous craniopharyngioma (n = 1), oligoastrocytoma WHO grade 2 (n = 1), oligodendroglioma dysembryoplastic (n = 1), primitive neuroectodermal tumor (medulloblastoma) (n = 1), vascular spindle cell mesenchymal neoplasm (n = 1), and vascularized mesenchymal tumor (n = 1). (B) Infratentorial tumors: desmoplastic/nodular medulloblastoma (n = 13), pilocytic astrocytoma (n = 10), anaplastic ependymoma (n = 7), anaplastic astrocytoma (n = 7), diffuse fibrillary astrocytoma (n = 3), ependymoblastoma (n = 1), ependymoma WHO grade 2 (n = 1), and medulloblastoma large cell/anaplastic tumor (n = 1). (C) Supra- and infratentorial tumors: arachnoid cyst (n = 9), anaplastic glioma (n = 3), gliosarcoma (n = 2), and meningioma (n = 1). (D) Tumors of specific location: brain stem glioma (n = 3), choroid plexus carcinoma (n = 2), chordoma (n = 2), and pineoblastoma (n = 2). There were no cases of intraventricular tumors in our sample. These histological results were obtained before the tumors were selected, based on the inclusion/exclusion criteria.

2.5. Imaging studies

2.5.1. Image acquisition and calculation of ADC values

Brain MRI was performed on a 3-T whole-body system (Magnetom Skyra; Siemens Medical Solutions, Erlangen, Germany) with a 20-channel phased array head coil. The imaging protocol included axial T1-weighted images before and after administration of the intravenous contrast agent. Further axial echo planar diffusion-weighted images were obtained for all patients. Acquisition parameters were as follows: repetition time (TR) = 5154 ms; echo time (TE) = 110 ms; flip angle = 90°; field of view = 22 cm; number of excitations = 5; acquired resolution = 1.5 × 1.5 × 5 mm]. Two b-values of 0 and 1000s/mm^2 were used. Diffusion gradients were applied in the z, y, and x directions. ADC maps (mm^2/s) were automatically calculated by built-in scanner software.

2.5.2. Regions of interest

Different regions of interest (ROIs) settings and ADC analyses were performed as described below:

1 The whole tumor was defined based on contrast-enhanced T1-weighted and diffusion-weighted imaging (DWI)/ADC images.
2 The ROIs were manually marked onto ADC maps by delineating/drawing a line around the entire lesion, using a single-voxel technique by segmenting the whole mass (Fig. 1, panels 1-B, 2-B, 3-B).
3 Additional ROIs were marked by delineating/drawing a line around the enhanced part of the lesion that had been defined based on contrast-enhanced T1-weighted and DWI/ADC images. (Fig. 1, panels 1-C, 2-C, 3-C).
4 The tumor was only evaluated, based on the mean ADC value of the aforementioned readings, by utilizing the computed mean of the ADCmin and the maximum apparent diffusion coefficient (ADCmax) to obtain an average dataset of encountered tumoral properties.
5 Based on the WHO criteria [19], histologically diagnosed WHO III and IV tumors were defined as “high-grade tumors” and WHO I and II tumors were defined as “low-grade tumors.”

Three board-certified radiology specialists performed this analysis, and three neuroradiology consultants reviewed their data by sampling the measures with subsequent agreement on all results. Cronbach’s alpha coefficient was 0.949 (i.e., 94.9%), which indicated adequate

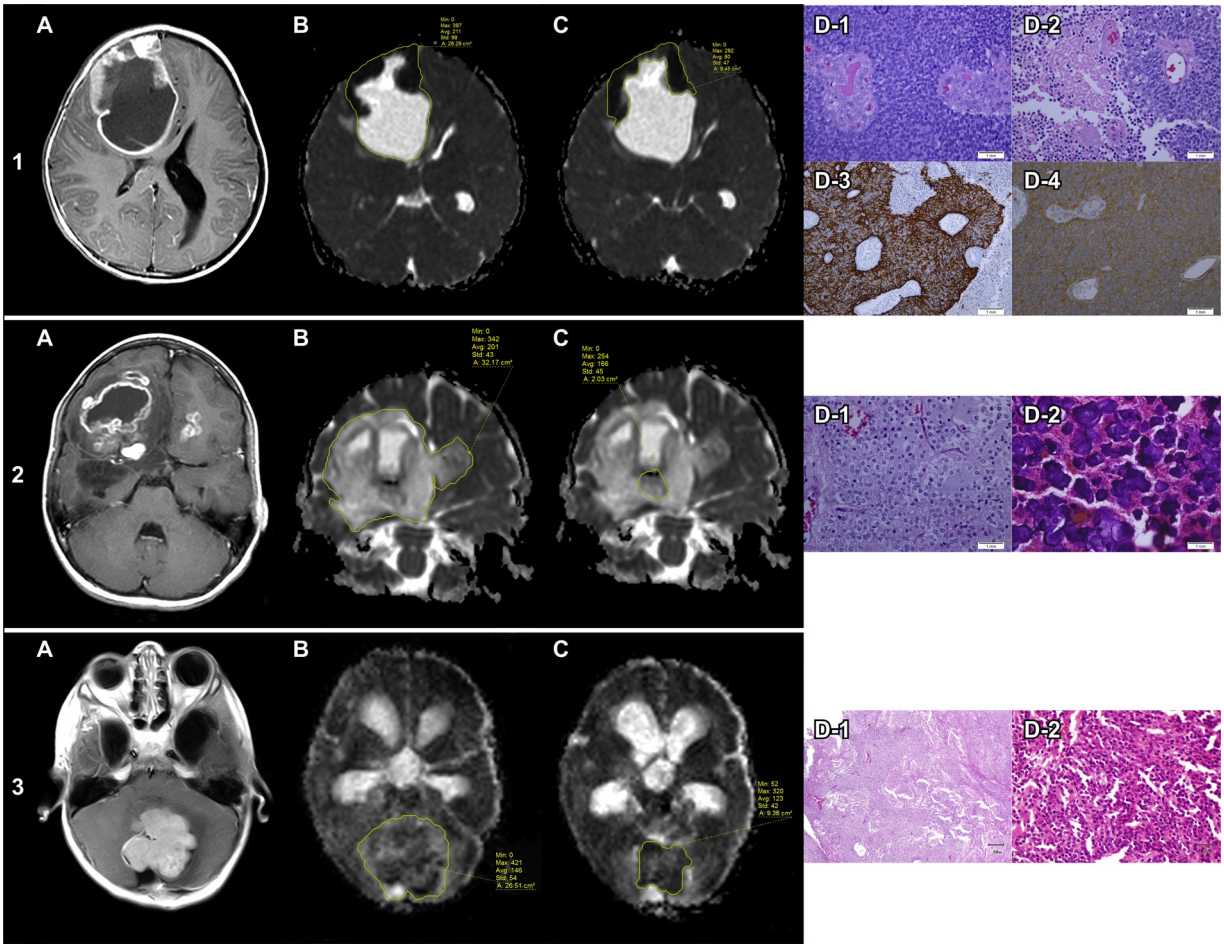

Fig. 1. Measurements of ADC values of whole lesions and contrast-enhancing tumor regions and the values' relationship with the histopathological findings that provided a provisional diagnosis.

1. A 10-year-old female patient. (a) T1-weighted postcontrast magnetic resonance imaging shows a complex contrast-enhanced cystic lesion in the right middle frontal gyrus with a mass effect upon the ipsilateral ventricle and a midline shift toward the left side. (b) The ADC value of the complex cystic lesion is $0.211 \times 10^{-3}\,mm^2/s$. (c) The ADC value of the solid component is $80 \times 10^{-3}\,mm^2/s$. (d) Histopathological analysis reveals small undifferentiated cells with hyperchromatic nuclei and scanty cytoplasm arranged around blood vessels with microvascular proliferation, aggressive behavior, and extensive necrosis (D1, D2) (H &E, × 400). The IHC analysis reveals positive immunoreactivity for GFAP (D3) and synaptophysin (D4) (IHC, ×400). These findings are consistent with ependymoblastoma versus anaplastic ependymoma, which lies within the computed range of ependymal tumor ADC values.

2. A 16-year-old female patient. (a) The T1-weighted postcontrast MRI shows a complex cystic lesion with necrotic portions that involve the bilateral frontal region and right temporal region. (b) The ADC value of the complex lesion is $201 \times 10^{-3}\,mm^2/s$. (c) The ADC value of the solid component is $166 \times 10^{-3}\,mm^2/s$. (d) Histopathological analysis reveals "boxed in" cells with cytoplasmic clearing and "chicken wire" vasculature (D1) with extensive calcification (D2) (H&E, × 400). These features are consistent with oligodendroglioma and the ADC value lies within the computed range of diffuse astrocytic and oligodendroglial tumor ADC values.

3. A 9-year-old-male patient. (a) The T1-weighted post-contrast MRI shows a lobulated, contrast-enhancing solid lesion within the posterior fossa that caused a mass effect upon the fourth ventricle with obstructive hydrocephalus. (b) The ADC value of the lesion is $146 \times 10^{-3}\,mm^2/s$. (c) The ADC value of the solid component is $123 \times 10^{-3}\,mm^2/s$. (d) Histopathological analysis reveals a highly cellular tumor mass of undifferentiated cells with variable growth patterns. The mass includes small, round to carrot–shaped uniform cells with hyperchromatic nuclei and wispy cytoplasm (D2), often with a distinct fibrillary background composed of cellular processes consistent with medulloblastoma. The ADC value lies within the computed range of embryonal tumor ADC values (D1, D2)

Abbreviations: ADC, apparent diffusion coefficient; GFAP, glial fibrillary acidic protein; H&E, hematoxylin and eosin; IHC, immunohistochemistry; MRI, magnetic resonance imaging

reliability. For the sake of consistency, the results were recorded as the mean of the two nearest values per ADC value. The kappa test was conducted to evaluate the obtained agreement significance (> 80%).

2.6. Statistical analysis

Statistical analysis was performed by using SPSS 21.0 version and MINITAB 17.0 version. Whole-lesion ADC values are presented as the median and range because the values were not normally distributed. Comparisons among tumor types were performed by using the Kruskal–Wallis test. The mean and standard deviation were used for the presentation of contrast-enhancing ADC values (i.e., ADC values of the contrast-enhancing tumor regions), and comparisons were performed by using analysis of variance (ANOVA). Statistical significance was set at p-values < 0.05.

2.7. Ethical statement

This retrospective cohort study was approved by the institutional review board of the XXX University and the need for informed consent was waived. For this type of study formal consent is not required.

3. Results

3.1. Descriptive analysis of the study patients

We retrospectively reviewed 80 cases with a histopathologically confirmed PBT. The mean age of the children was 11.03 ± 6.61 years, with a predominance of males (78 [66.7%]) over females (39 [33.3%]). Axial relationships revealed that the majority of cases (73 [62.4%]) were intra-axial tumors, followed by extra-axial (26 [22.2%]) and interventricular tumors (18 [15.4%]). There was a slight predilection for the left side vs. the right side (43 [36.8%] vs. 39 [33.3%]). The frontal lobe was predominantly involved (38 [32.5%]), followed by the temporal lobe (25 [21.4%]). The vast majority of cases had solitary lesions (103 [88.0%]), but multicentric/multifocal lesions were also observed (14 [12.0%]). Tumor growth characteristics, such as central necrosis (63 [53.8%]), herniation (37 [31.6%]), hemorrhage (16 [12.8%]), and midline shifts (50 [42.7%]) were observed. The majority of lesions (93 [79.5%]) showed no restriction on diffusion sequences.

3.2. Preoperative signal analysis

Compared with gray matter signal intensity, the T2-weighted signal analysis showed high signal intensity in approximately one-half of cases (53 [45.3%]). The remaining lesions showed variable signal intensities ranging from intermediate intensity (10 [8.5%]) to low (30 [25.6%]) or ISO (1 [0.9%]) signal intensity. The diffusion-weighted signal analysis showed variable diffusions, and ranged from high diffusion (19 [16.2%]) to intermediate (7 [6.0%]), ISO (1 [0.9%]), or low (48 [41.0%]) diffusion. Reformatted ADC signal analysis showed different values ranging from high signal (28 [23.9%]) to intermediate (5 [4.3%]), ISO (2 [1.7%]), or low (59 [50.4%]) signal.

3.3. Brain tumor statistics

Whole-lesion ADC values were significantly different among the types of PBTs (p = 0.030, Kruskal–Wallis test; Table 1). Fisher's pairwise comparisons (Fig. 2) revealed significant differences ($p < 0.05$) between embryonal tumors and meningiomas. There were also significant differences between diffuse astrocytic and oligodendroglial tumors and meningiomas. ADC values were more scattered in embryonal tumors as well as in diffuse astrocytic and oligodendroglial tumors (Fig. 3). The dispersion of ADC data was lower in higher-grade tumors than in low-grade tumors. There were no significant differences in ADC values of the contrast-enhancing tumor regions between the types of PBTs (p = 0.878; Table 2, Fig. 4).

Whole-lesion ADC values ranged 0.225–1.240 $\times 10^{-3}$ mm^2/s for ependymal tumors, 0.107–1.571 $\times 10^{-3}$ mm^2/s for embryonal tumors, 0.1065–2.37801 $\times 10^{-3}$ mm^2/s for diffuse astrocytic and oligodendroglial tumors, 0.5220–0.7840 $\times 10^{-3}$ mm^2/s for other astrocytic tumors, and 0.1530–0.8160 $\times 10^{-3}$ mm^2/s for meningiomas.

Table 1
Comparison of whole-lesion ADC values across different PBT types.

PBT type as per WHO classification (20) (N)	ADC Median (range), $\times 10^{-3}$ mm^2/s	P value
Ependymal tumors (5)	0.595 (0.225–1.240)	0.030*
Embryonal tumors (12)	1.016 (0.107–1.571)	
Diffuse astrocytic and oligodendroglial tumors (49)	1.0110 (0.1065–2.37801)	
Other astrocytic tumors (7)	0.6790 (0.5220–0.7840)	
Meningiomas (7)	0.2950 (0.1530–0.8160)	

Abbreviations: ADC, apparent diffusion coefficient; PBT, pediatric brain tumor; WHO, World Health Organization.

* Statistically significant by KruskalWallis test. Statistical significance was set at p-values < 0.05.

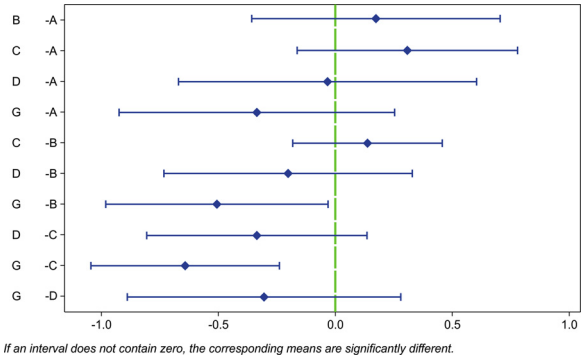

Fig. 2. Fisher's pairwise comparisons of whole-lesion ADC values between different PBT types.
Fisher's pairwise comparisons show a significant difference between embryonal tumors and meningiomas and between diffuse astrocytic and oligodendroglial tumors and meningiomas. If an interval does not contain zero, the corresponding means are significantly different
A = "ependymal tumors", B = "embryonal tumors", C = "diffuse astrocystic and oligodendroglial tumors", D = "other astrocystic tumors", G = "meningiomas".
Abbreviations: ADC, apparent diffusion coefficient; PBT, pediatric brain tumor

4. Discussion

Diffusion-weighted imaging is a key sequence for the diagnosis of cerebral infarction, abscesses, brain neoplasms, etc. In recent years, DWI has been used in the diagnosis of brain tumors with promising and sometimes controversial results [17,20,21]. In this study, we first hypothesized that, because tissue water mobility is intimately and directly dependent on tissue microstructure, tumor heterogeneity would manifest as an intervoxel difference of the calculated ADC value. We found that ADC may be useful in the differential diagnosis of PBT because it allowed the discrimination between five types of PBTs.

Our findings are in line with those of previous studies that proposed that the calculated ADC value can be used to differentiate between primitive neuroectodermal tumor/medulloblastoma and other supra- and infratentorial tumors [12,14]. Pilocytic astrocytomas have significantly higher average ADC values than those of ependymomas and medulloblastomas; however, a clear cutoff point to differentiate between ependymomas and medulloblastomas has not been established [13].

Diffusion-weighted imaging and ADC maps have been correlated with tumor grade, and their relationship with tumor cellularity has been established [20,22]. For instance, Murakami et al. [22] demonstrated that regions exhibiting ADCmin corresponded to the foci of the highestgrade gliomas and that high ADC difference values (i.e., between the upper limit and ADCmin) strongly corresponded with overall high-grade lesions rather than low-grade lesions. Porto et al. [20] retrospectively studied 36 PBTs, divided them into low grade and high grade, measured the ADCmin cutoff and average ADC values, and compared these values between the low-grade and high-grade tumors. Some attempts were made to identify ADC value ranges that could be used to predict a particular tumor type. Rumboldt et al. [17] studied 32 pediatric cerebellar tumors and identified cutoff points specifically for juvenile pilocytic astrocytomas, medulloblastomas, and atypical teratoid/rhabdoid tumors. In addition, Gimi et al. [18] studied 79 pediatric cerebellar tumors and clarified the potential thresholds for diagnosing various types of cerebellar tumors—specifically, pilocytic astrocytomas, medulloblastomas, ependymomas, and seven atypical teratoid/rhabdoid tumors. Our study is novel in that it extended the investigations to supra- and infratentorial tumors, rather than being restricted to the posterior fossa or cerebellar tumors, and addressed

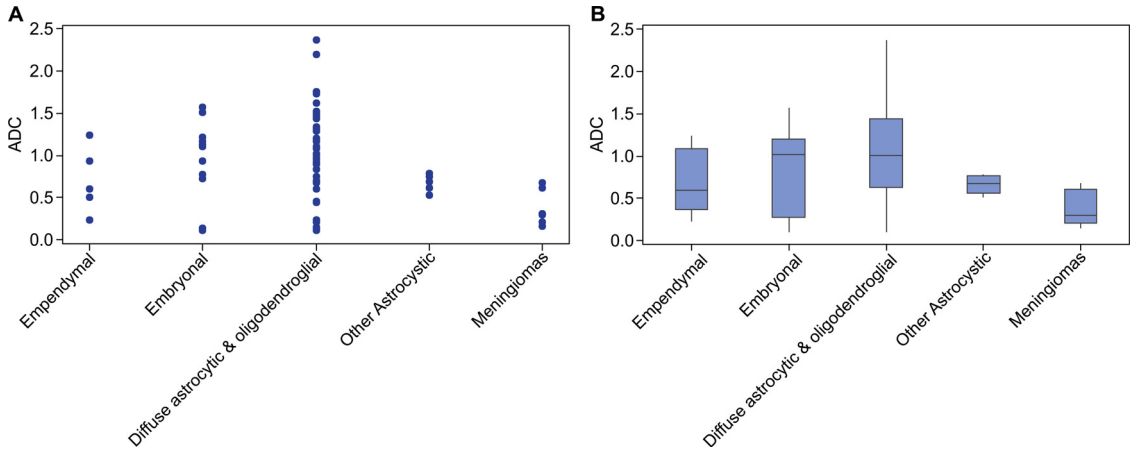

Fig. 3. Distribution of mean ADC values for different types of PBTs.
(a) The scatter plot shows the ADC data are more scattered for embryonal and diffuse astrocytic and oligodendroglial tumors. (b) The box plot shows less dispersion for meningiomas, compared with other tumors
Abbreviations: ADC, apparent diffusion coefficient; PBTs, pediatric brain tumors

some rare types of PBTs such as meningiomas and oligodendroglial tumors that have not been evaluated previously. Moreover, we investigated embryonal tumors such as medulloblastomas and neuroblastomas.

Some studies contradict our findings and previous findings. In 56 patients, Kono et al. [7] examined the solid portions and peritumoral hyperintense areas with four main types of tumors (i.e., glioblastoma, low-grade astrocytoma, metastatic tumor, and meningioma) and concluded that ADC values could not be reliably applied to predict the tumor type in individual patients [7]. Zonari et al. [23] found no significant difference in the minimum ADCs of low-grade versus high-grade glial tumors. Catalaa et al. [24] reported that ADCs could not be used to distinguish between different tumor grades. Their conclusions may be explained by the fact that they used methodology and sample sizes that differed from those in the aforementioned studies.

In general, few studies exist on the diffusion-weighted image characteristics of pediatric patients. Previous reports have been limited by small sample sizes or by their focus on particular types of PBT with characteristic anatomical locations, especially those in the posterior fossa and cerebellar regions [15–17,25]. Other studies have focused solely on grading a single type of tumor [22,26,27], or have proposed a specific histogram pattern that defined a particular type of PBT by using mathematical equations, which suggests the ability to use ADC maps to predict certain types of PBTs or their current grade [21,28]. Surgical biopsy has significant risks in morbidity and mortality, whereas obtaining a definitive diagnosis and discriminating between tumors by using DWI may be possible. However, ADC cutoff values need to be established.

It is recognized that an indistinct type of tumor (e.g., glioma) demonstrates a broad range of histological features that change from low- to high-grade; thus, the calculated ADCs within a given frame can vary

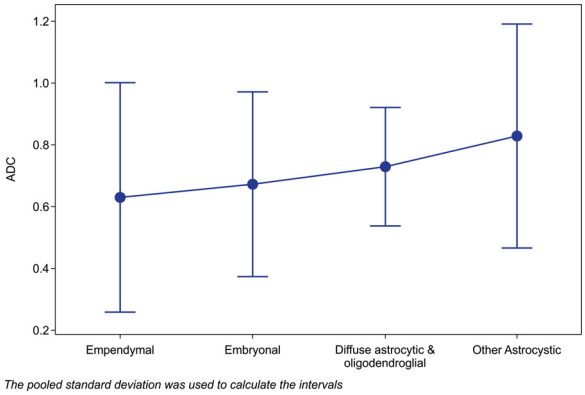

Fig. 4. Median ADC values of contrast-enhanced tumor regions for different types of PBTs.
The plot chart with 95% confidence intervals shows that ADC values of contrast-enhanced tumor regions are insufficient for differentiating between PBT types (p = 0.878). The pooled standard deviation was used to calculate the intervals

widely between different regions of a tumor. An ADC derived from regional ROIs will likely obscure tissue heterogeneity in highly cellular tumors such as high-grade gliomas [23]. Nevertheless, the selection of a localized area within a tumor can differ subjectively and may be prone to sampling bias [29,30].

A more objective approach that is superior to manual placement of regional ROIs would be to analyze the ADC value of the entire volume of the lesion. This approach should provide quantitative information about mixed tissue cellularity and reflect the characteristics of the

Table 2
Comparison of ADC values of contrast-enhancing PBT regions in T1-weighted images.

PBT type as per WHO classification (20) (N)	ADC		P value
	Mean (SD)	95% CI	
Ependymal tumors (5)	0.631 (0.45)	0.256–1.007	0.878
Embryonal tumors (12)	0.674 (0.30)	0.367–0.981	
Diffuse astrocytic and oligodendroglial tumors (49)	0.7316 (0.35)	0.537–0.925	
Other astrocytic tumors (7)	0.825 (0.42)	0.449–1.201	

Abbreviations: ADC, apparent diffusion coefficient; CI, confidence interval; PBT, pediatric brain tumor; SD, standard deviation; WHO, World Health Organization.
Note: Meningiomas are non-enhancing lesions; therefore, they were not included in this analysis.

tumor as a whole. Our study combined this method with analytical histograms, which have been used to determine cutoff points for ADC values. These cutoff points could be used clinically to discriminate between multiple groups of PBTs and to evaluate the diagnostic performance of ADC maps at b-values of the standard 1000s/mm2 and as high as 3000 s/mm2. This has been implemented in a recently validated WHO classification system [19], which represents a conceptual and practical advance over its 2007 predecessor [31].

The latest WHO classification system uses molecular parameters and histopathology to define many tumor entities, and thus formulating a structured standard of how brain tumors should be diagnosed, based on their genetic and molecular backgrounds. Based on the new brain tumor classification [19], implementing molecular validations in the diagnostic process is more reliable than histology in predicting survival and tumor behavior. Witt et al. [32] demonstrated that utilizing molecular data is useful for distinguishing between rare medulloblastoma subgroups (e.g., WNT) with a similar prognosis as pilocytic astrocytomas, whereas histological grading of posterior fossa ependymomas is not as useful as molecular data in distinguishing between subgroups.

In pediatric central nervous system tumors, histological diagnosis of oligodendroglioma is challenging. The diagnosis of oligodendroglioma and anaplastic oligodendroglioma requires the presence of the isocitrate dehydrogenase (IDH) gene family mutation and whole-arm losses of both 1p and 19q. This criterion was validated in our included samples of this type. However, most tumors in childhood that histologically resemble oligodendroglioma often do not demonstrate isocitrate dehydrogenase gene family mutation and 1p/19q codeletion [19]. Oligodendrogliomas are very rare in children, and some authors believe they are virtually absent.

These diagnostic criteria are poorly applicable in clinical practice. The present study sought to determine cutoff values that could be rapidly and reliably implemented. Our results indicated a significant difference in ADC values among the included types of PBTs, with a Pearson's correlation coefficient of 0.030 (Table 1). This statistical difference was confirmed on analytical histograms (Figs. 2–4). By contrast, the ADC values of contrast-enhancing tumor regions did not adequately differentiate between tumor types ($p = 0.878$).

Our study was limited in that it was a retrospectively designed cohort study. We advocate for prospective application of our methodology in a sufficient sample size. The whole tumor was determined, based on contrast-enhanced T1-weighted and DWI/ADC images. However, a few of the encountered tumors were not enhanced and other tumors may have been variable in time enhancement. In fact, the evidence of the Response Assessment in Pediatric Neuro-Oncology (RAPNO) criteria for low-grade gliomas ($n = 4$ in this study) does not suggest using post-contrast sequences to define the tumor burden, but the T2WI [33].

Whole-lesion ADC values may potentially be used to discriminate between the PBT types included in this study, which suggests that the ADC can be used as a diagnostic criterion. This method is easily applied because ADC can be calculated using automated software. Using this method only is a possible approach. However, multiparametric correlations is a better approach. Apparent diffusion coefficient, more importantly, could provide a fast, provisional differential diagnosis without requiring biopsy, which requires lengthy histopathological analysis to obtain a precise diagnosis.

The ADC is an easily calculated parameter that could be used to discriminate between five types of PBTs—namely, meningiomas, diffuse astrocytic and oligodendroglial tumors, ependymal tumors, and embryonal tumors. The conventional method requires collecting a biopsy specimen, sending it to a histopathology laboratory for analysis, and awaiting the results. By contrast, the proposed cutoff values of ADC ranges may provide a rapid diagnosis and aid in excluding other types of tumors. Even with an optimized technique for determining the objective ADCmin in each tumor, our study was limited by a true overlap between diffusion characteristics. The overlap is accounted for by technical difficulties in ADC measurement (in small, hemorrhagic, or calcified tumors) and by variations in tumor pathology. The application of an ADC diagnostic criterion would reduce the need for spectroscopic analysis. However, further research is needed to implement ADC in the differential diagnosis of PBT.

5. Conclusions

The ADC is an easily calculated parameter that could be used to discriminate between five types of PBTs—namely, meningiomas, diffuse astrocytic and oligodendroglial tumors, ependymal tumors, and embryonal tumors. The conventional method requires collecting a biopsy specimen, sending it to a histopathology laboratory for analysis, and awaiting the results. By contrast, the proposed cutoff values of ADC ranges may provide a rapid diagnosis and aid in excluding other types of tumors. Even with an optimized technique for determining the objective ADCmin in each tumor, our study was limited by a true overlap between diffusion characteristics. The overlap is accounted for by technical difficulties in ADC measurement (in small, hemorrhagic, or calcified tumors) and by variations in tumor pathology. The application of an ADC diagnostic criterion would reduce the need for spectroscopic analysis. However, further research is needed to implement ADC in the differential diagnosis of PBT.

Declarations of interest

None.

Ethical approval

This retrospective cohort study was approved by the institutional review board of the Imam Abdulrahman Bin Faisal University (Approval number: IRB-2014-01-357), and the need for informed consent was waived.

Funding

This research did not receive any specific grant from funding agencies in the public, commercial, or not-for-profit sectors.

Acknowledgements

We would like to thank Dr. Eman Debawy and Mr. Abdulaziz AlSaedi for their contribution in data collection.

References

[1] E. Ward, C. DeSantis, A. Robbins, B. Kohler, A. Jemal, Childhood and adolescent cancer statistics, 2014, CA Cancer J. Clin. 64 (2) (2014) 83–103, https://doi.org/10.3322/caac.21219.
[2] T.A. Dolecek, J.M. Propp, N.E. Stroup, C. Kruchko, CBTRUS statistical report: primary brain and central nervous system tumors diagnosed in the United States in 2005–2009, Neuro Oncol. 14 (2012) v1-49.
[3] A.L. Wiens, E.M. Hattab, The pathological spectrum of solid CNS metastases in the pediatric population, J. Neurosurg. Pediatr. 14 (2014) 129–135, https://doi.org/10.3171/2014.5.PEDS13526.
[4] R. Bammer, Basic principles of diffusion-weighted imaging, Eur. J. Radiol. 45 (2003) 169–184.
[5] G.S. Young, Advanced MRI of adult brain tumors, Neurol. Clin. 25 (2007) 947–973.
[6] M. Raisi-Nafchi, F. Faeghi, A. Zali, H. Haghighatkhah, J. Jalal-Shokouhi, Preoperative grading of astrocytic supratentorial brain tumors with diffusion-weighted magnetic resonance imaging and apparent diffusion coefficient, Iran. J. Radiol. 13 (2016) e30426.
[7] K. Kono, Y. Inoue, K. Nakayama, M. Shakudo, M. Morino, K. Ohata, K. Wakasa, R. Yamada, The role of diffusion-weighted imaging in patients with brain tumors, Am. J. Neuroradiol. 22 (2001) 1081–1088.
[8] K. Krabbe, P. Gideon, P. Wagn, U. Hansen, C. Thomsen, F. Madsen, MR diffusion imaging of human intracranial tumours, Neuroradiology 39 (1997) 483–489.
[9] M. Wilke, A. Eidenschink, S. Müller-Weihrich, D.P. Auer, MR diffusion imaging and 1H spectroscopy in a child with medulloblastoma, Acta Radiol. 42 (2001) 39–42.
[10] P. Kan, J.K. Liu, G. Hedlund, D.L. Brockmeyer, M.L. Walker, J.R. Kestle, The role of diffusion-weighted magnetic resonance imaging in pediatric brain tumors, Childs

Nerv. Syst. 22 (2006) 1435–1439.
[11] L. Astrakas, S. Ye, M. Zarifi, F. Makedon, A.A. Tzika, The clinical perspective of large scale projects: a case study of multiparametric MR imaging of pediatric brain tumors, Oncol. Rep. 15 (2006) 1065–1070.
[12] K.M. Gauvain, R.C. McKinstry, P. Mukherjee, A. Perry, J.J. Neil, B.A. Kaufman, R.J. Hayashi, Evaluating pediatric brain tumor cellularity with diffusion-tensor imaging, AJR Am. J. Roentgenol. 177 (2001) 449–454.
[13] E. Erdem, R.A. Zimmerman, J.C. Haselgrove, L.T. Bilaniuk, J.V. Hunter, Diffusion-weighted imaging and fluid attenuated inversion recovery imaging in the evaluation of primitive neuroectodermal tumors, Neuroradiology 43 (2001) 927–933.
[14] F. Yamasaki, K. Kurisu, K. Satoh, K. Arita, K. Sugiyama, M. Ohtaki, J. Takaba, A. Tominaga, R. Hanaya, H. Yoshioka, S. Hama, Apparent diffusion coefficient of human brain tumors at MR imaging, Radiology 235 (2005) 985–991.
[15] J.F. Schneider, S. Confort-Gouny, A. Viola, Y. Le Fur, P. Viout, M. Bennathan, F. Chapon, D. Figarella-Branger, P. Cozzone, N. Girard, Multiparametric differentiation of posterior fossa tumors in children using diffusion-weighted imaging and short echo-time 1H-MR spectroscopy, J. Magn. Reson. Imaging 26 (2007) 1390–1398.
[16] J.L. Jaremko, L.B. Jans, L.T. Coleman, M.R. Ditchfield, Value and limitations of diffusion-weighted imaging in grading and diagnosis of pediatric posterior fossa tumors, AJNR Am. J. Neuroradiol. 31 (2010) 1613–1616.
[17] Z. Rumboldt, D.L. Camacho, D. Lake, C.T. Welsh, M. Castillo, Apparent diffusion coefficients for differentiation of cerebellar tumors in children, AJNR Am. J. Neuroradiol. 27 (2006) 1362–1369.
[18] B. Gimi, K. Cederberg, B. Derinkuyu, L. Gargan, K.M. Koral, D.C. Bowers, K. Koral, Utility of apparent diffusion coefficient ratios in distinguishing common pediatric cerebellar tumors, Acad. Radiol. 19 (2012) 794–800.
[19] D.N. Louis, A. Perry, G. Reifenberger, A. von Deimling, D. Figarella-Branger, W.K. Cavenee, H. Ohgaki, O.D. Wiestler, P. Kleihues, D.W. Ellison, The 2016 World Health Organization classification of tumors of the central nervous system: a summary, Acta Neuropathol. 131 (2016) 803–820.
[20] L. Porto, A. Jurcoane, D. Schwabe, M. Kieslich, E. Hattingen, Differentiation between high and low grade tumours in paediatric patients by using apparent diffusion coefficients, Eur. J. Paediatr. Neurol. 17 (2013) 302–307.
[21] J.G. Bull, D.E. Saunders, C.A. Clark, Discrimination of paediatric brain tumours using apparent diffusion coefficient histograms, Eur. Radiol. 22 (2012) 447–457.
[22] R. Murakami, T. Hirai, T. Sugahara, H. Fukuoka, R. Toya, S. Nishimura, M. Kitajima, T. Okuda, H. Nakamura, N. Oya, J. Kuratsu, Y. Yamashita, Grading astrocytic tumors by using apparent diffusion coefficient parameters: superiority of a one- versus two-parameter pilot method, Radiology 251 (2009) 838–845.
[23] P. Zonari, P. Baraldi, G. Crisi, Multimodal MRI in the characterization of glial neoplasms: the combined role of single-voxel MR spectroscopy, diffusion imaging and echoplanar perfusion imaging, Neuroradiology 49 (2007) 795–803.
[24] I. Catalaa, R. Henry, W.P. Dillon, E.E. Graves, T.R. McKnight, Y. Lu, D.B. Vigneron, S.J. Nelson, Perfusion, diffusion and spectroscopy values in newly diagnosed cerebral gliomas, NMR Biomed. 19 (2006) 463–475.
[25] K. Koral, R. Alford, N. Choudhury, M. Mossa-Basha, L. Gargan, B. Gimi, A. Gao, S. Zhang, D.C. Bowers, K.M. Koral, I. Izbudak, Applicability of apparent diffusion coefficient ratios in preoperative diagnosis of common pediatric cerebellar tumors across two institutions, Neuroradiology 56 (2014) 781–788.
[26] E.J. Lee, S.K. Lee, R. Agid, J.M. Bae, A. Keller, Preoperative grading of presumptive low-grade astrocytomas on MR imaging: diagnostic value of minimum apparent diffusion coefficient, AJNR Am. J. Neuroradiol. 29 (2008) 1872–1877.
[27] S. Higano, X. Yun, T. Kumabe, M. Watanabe, S. Mugikura, A. Umetsu, A. Sato, T. Yamada, S. Takahashi, Malignant astrocytic tumors: clinical importance of apparent diffusion coefficient in prediction of grade and prognosis, Radiology 241 (2006) 839–846.
[28] D.J. Tozer, H.R. Jäger, N. Danchaivijitr, C.E. Benton, P.S. Tofts, J.H. Rees, A.D. Waldman, Apparent diffusion coefficient histograms may predict low-grade glioma subtype, NMR Biomed. 20 (2007) 49–57.
[29] S.F. Kralik, A. Taha, A.P. Kamer, J.S. Cardinal, T.A. Seltman, C.Y. Ho, Diffusion imaging for tumor grading of supratentorial brain tumors in the first year of life, AJNR Am. J. Neuroradiol. 35 (2014) 815–823.
[30] T. Pierce, P.G. Kranz, C. Roth, D. Leong, P. Wei, J.M. Provenzale, Use of apparent diffusion coefficient values for diagnosis of pediatric posterior fossa tumors, Neuroradiol. J. 27 (2014) 233–244.
[31] D.N. Louis, H. Ohgaki, O.D. Wiestler, W.K. Cavenee, P.C. Burger, A. Jouvet, B.W. Scheithauer, P. Kleihues, The 2007 WHO classification of tumours of the central nervous system, Acta Neuropathol. 114 (2007) 97–109.
[32] H. Witt, S.C. Mack, M. Ryzhova, S. Bender, M. Sill, R. Isserlin, et al., Delineation of two clinically and molecularly distinct subgroups of posterior fossa ependymoma, Cancer Cell 20 (2011) 143–157, https://doi.org/10.1016/j.ccr.2011.07.007.
[33] M.J. Van den Bent, J.S. Wefel, D. Schiff, M.J. Taphoorn, K. Jaeckle, L. Junck, et al., Response assessment in neuro-oncology (a report of the RANO group): assessment of outcome in trials of diffuse low-grade gliomas, Lancet Oncol. 12 (2011) 583–593, https://doi.org/10.1016/S1470-2045(11)70057-2.